Fluorescent Flipper Probes: Comprehensive Twist Coverage

Strakova, Karolina; Poblador Bahamonde, Amalia Isabel; Sakai, Naomi; Matile, Stefan

How to cite

STRAKOVA, Karolina et al. Fluorescent Flipper Probes: Comprehensive Twist Coverage. In: Chemistry - A European Journal, 2019, vol. 25, n° 65, p. 14935–14942. doi: 10.1002/chem.201903604

This publication URL: https://archive-ouverte.unige.ch/unige:126804
Publication DOI: 10.1002/chem.201903604

Fluorescent Flipper Probes: Comprehensive Twist Coverage

Karolina Strakova, Amalia I. Poblador-Bahamonde, Naomi Sakai, and Stefan Matile*[a]

[a] K. Strakova, Dr. A. Poblador-Bahamonde, Dr. N. Sakai, Prof. S. Matile

Department of Organic Chemistry

University of Geneva, Geneva, Switzerland

E-mail: stefan.matile@unige.ch

Homepage: www.unige.ch/sciences/chiorg/matile/

Supporting information for this article is given via a link at the end of the document.

Abstract: To image the membrane tension in living cells, planarizable push-pull probes have been introduced. The first operational probe is built around two dithieno[3,2-*b*:2',3'-*d*]thiophenes (DTTs) that are twisted out of co-planarity and polarized with donors and acceptors at either end. In this report, the chemical space available for the twisting of "flipper probes" is assessed comprehensively. The result is, not surprisingly, that every atom matters: Removal of one methyl group in the twist region yields probes that planarize already in solution and are thus less sensitive to membrane tension. Addition of one or more carbons in the same region hinders non-interfering probe alignment along lipid tails and thus partitioning into lipid bilayer membranes as well as mechanosensitivity. However, substitution of one methyl by an isosteric trifluoromethyl group in the twist region, achieved by quite substantial multistep organic synthesis, yields excitation maxima that shift over +100 nm to the red in response to increasing order of the surrounding membrane. This record red shift comes with record changes in fluorescence intensity and lifetime, high push-pull transition dipoles and high rotational barriers. Supported by distinct dependence on viscosity and twist of the push-pull probes, kinetic

competition between dark, fully twisted and bright, fully planarized relaxed excited states emerges as unifying origin of fluorescence quantum yields.

Introduction

The fluorescence imaging of physical forces in living systems in general and membrane tension in particular is a challenge in current biology that calls for solutions from chemistry.[1] Toward this end, we have introduced the concept of planarizable push-pull probes in 2012.[2] Inspired by the color change of lobsters during cooking,[3] the expectation is that the planarization of twisted probes in the ground state by physical forces from the environment will turn on the push-pull system and thus red shift the excitation maximum and increase fluorescence intensity, i.e., lifetime. Result of a quite extensive evolution over several years, the current best is Flipper-TR® **1** (Figure 1a).[4] It is composed of two dithienothiophene (DTT) "flippers". One electron-rich DTT with a formal sulfide and an electron-poor, highly fluorescent DTTO2 with a sulfone bridging the two thiophenes establish the primary push-pull system. The "sulfone bridge" is supported by an exocyclic cyano acceptor, the sulfide by a turn-on chalcogen-bonding ether donor.

In lipid bilayer membranes of increasing order, the excitation maximum of flipper **1** shifts to the red. This red shift is consistent with flipper planarization by an increasingly confining environment, in the ground state, in equilibrium. This mode of action differs from common fluorescent membrane probes that operate off-equilibrium in the excited state.[5] The red shift of the excitation of flipper **1** with increasing membrane order coincides with an increase of fluorescence intensity and lifetime. The latter is attractive for concentration-independent force imaging by FLIM (fluorescence lifetime imaging microscopy).[4,5] According to FLIM images of

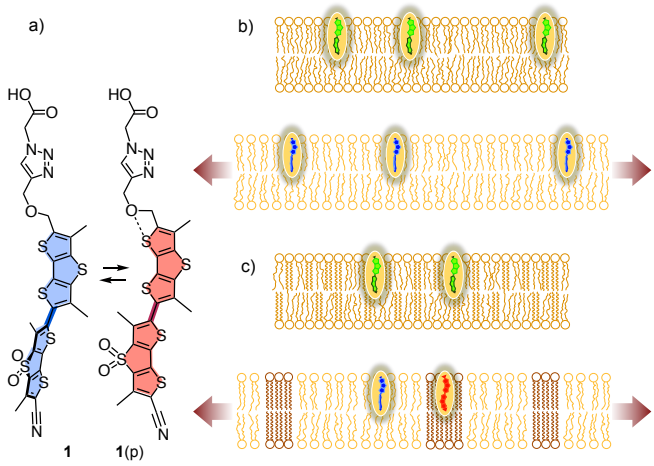

Figure 1. a) Planarization in the ground state of the original flipper probe **1** with increasing membrane order red shifts the excitation maximum and increases fluorescence lifetime. b) Decreasing lifetimes with increasing tension applied to homogeneous membranes is consistent with blue-shifting flipper deplanarization (blue) upon lipid decompression. c) Increasing lifetimes with increasing tension applied to heterogeneous membranes is consistent with tension-induced microdomain assembly and dominant response from red-shifted planarized flipper (red) in ordered microdomains.

1 in homogeneous lipid bilayer membranes, the application of tension is reported as linearly decreasing lifetimes, with slopes depending on the lipid composition.[6] This trend is consistent with flipper deplanarization upon lipid decompression (Figure 1b). In heterogeneous lipid bilayer membranes, the application of tension is reported as linearly increasing lifetimes. This trend is consistent with tension-induced microdomain assembly[7] and a dominant response from planarized flippers in highly-ordered, poorly stretchable microdomains (Figure 1c). Compatibility of this response with the imaging of membrane tension in plasma membrane, endo-lysosomes,

mitochondria and ER has been demonstrated.[8] As a result, flipper probes are increasingly used to address questions in mechanobiology that were beyond reach until now, including the functional relevance of tension-induced microdomain assembly and disassembly.[9] This experimental evidence for fluorescence imaging of physical forces in living cells called for the exploration of the chemical space around fluorescent flipper probe **1**. The objective of this study was to cover the twist region comprehensively.

Results and Discussion

Synthesis

Mechanophores **1**–**5** (Figure 2) were accessible through interesting multistep synthesis (Schemes 1, S1–S4). Following the procedure previously developed for flippers **1** and **5**,[10] flippers **4** and **3** with one more and one less carbon in the twist region were prepared from tetrabromothiophene **6**. Acylation with differently substituted aldehydes, e.g., **7** and **8**, ultimately resulted in the DTT scaffolds **9** and **10** with different β substituents. A cascade reaction of the acylation product **10** with thioacetate ethyl ester **11**, comprising an enolate addition to the carbonyls, dehydration, and substitution of the bromides of the central thiophenes by the thiol nucleophiles, afforded DTT scaffold **12**. Whereas DTT **13** (R = H)[11] was commercially available and used as received, the corresponding DTT **14** (R = Et) was then obtained by hydrolysis of the α esters in **12** followed by decarboxylation. Formylation of one of the free α positions of DTTs **13** and **14** followed by reduction and silyl protection of the primary alcohols yielded DTT donors **15** and **16**. Stille coupling with the previously reported DTTO2 acceptors **17** gave the hydrophobic flippers **3'** and **4'**. Headgroup modification following established Williamson ether synthesis and CuAAC cycloaddition yielded the final flipper amphiphiles **3** and **4**.

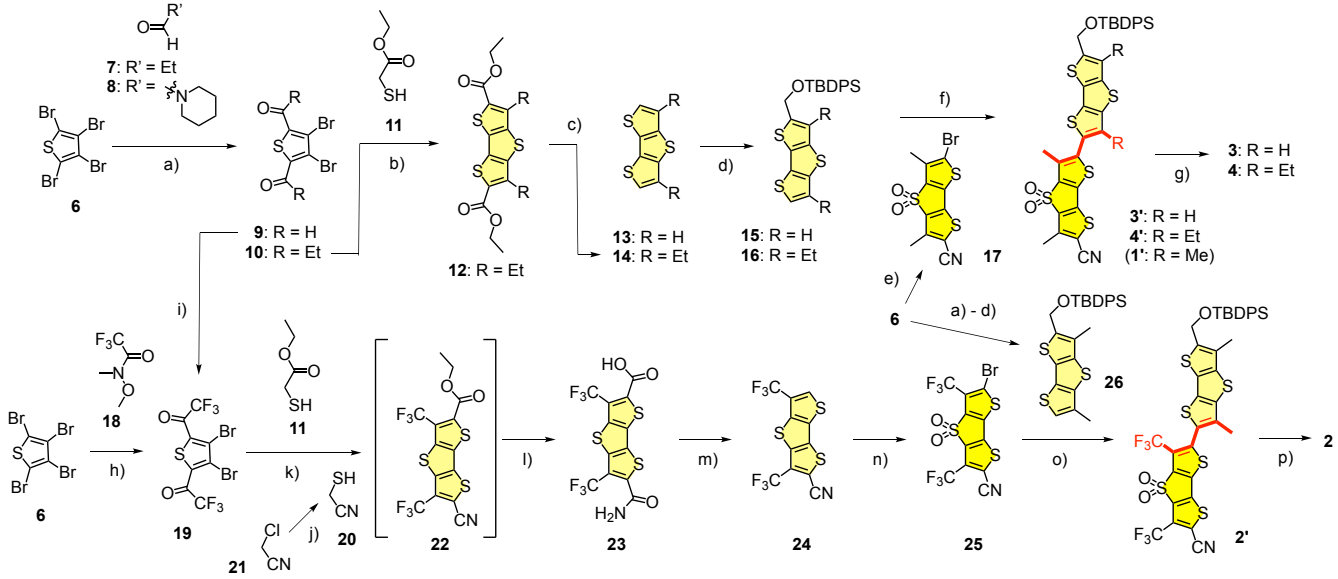

Scheme 1. a) R = H: 1. BuLi, THF, -78 °C – rt, 50 min; 2. **8**, -78 °C – rt, overnight, 60%; R = Et: 1. BuLi, -78 °C, 15 min; 2. **7**, rt, 30 min, 74%; 3. $Na_2Cr_2O_7 \cdot 2H_2O$, H_2SO_4, acetone, rt, overnight, 50%; b) K_2CO_3, EtOH, 78 °C, 30 min, 82%; c) 1. KOH, EtOH, 78 °C, overnight; 2. 1 M HCl, water, rt, 5 min, quant.; 3. Ag_2CO_3, AcOH, DMSO, 120 °C, overnight, 80%; d) 1. $POCl_3$, DMF, 3 – 4 h, 50 – 60 °C, 69 – 84%; 2. $NaBH_4$, DMF, 70 °C, 2 h; 3. imidazole, TBDPS-Cl, DMF, rt, overnight, 74 – 81% over 2 steps; e) as in ref. [2b]; f) 1. BuLi, THF, -78 °C, 10 min; 2. Bu_3SnCl, THF, -78 °C – rt, 20 min; 3. $Pd(PPh_3)_4$, **17**, DMF, 75 °C, overnight, 48 – 72% over 3 steps; g) 1. TBAF, THF, rt, 30 min, 81 – 88%; 2. NaH, propargyl bromide, THF, DMF, 0 °C – rt, 30 min, 60 – 89%; 3. R = H: tert-butyl 2-azidoacetate, $CuSO_4 \cdot 5H_2O$, Na-ascorbate, TBTA, CH_2Cl_2, H_2O, rt, 24 h, 53%; R = Et: 2-azidoacetic acid, $CuSO_4 \cdot 5H_2O$, Na-ascorbate, TBTA, CH_2Cl_2, H_2O, rt, 30 min, 86%; 4. R = H: KOH, MeOH/water (2:1), rt, 30 min, 33%; h) 1. BuLi, THF, -78 °C, 15 min; 2. **18**, 78 °C – rt, 2.5 h, 63%; i) 1. $TMSCF_3$, CsF, DME, 0 °C, 30 min; 2. 3M HCl, 0 °C − rt, 80 min, 75% over 2 steps; 3. DMP, CH_2Cl_2, 0 °C – rt, 3 h, 72%; j) 1. thioacetic acid, Et_3N, CH_2Cl_2, -20 °C – rt, 1 h; 2. Amberlyst® 15, MeOH, 65 °C for 24 h and rt for 12 h, 85%; k) K_2CO_3, EtOH,

70 °C, 2 h, not isolated; l) KOH, EtOH, –78 °C, 3 h, 22% over k) and l) (9% when started from fully hydrated **19**); m) 1. Ag_2CO_3, AcOH, DMSO, 120 °C, 3 h, 80%; 2. $POCl_3$, 106 °C, 4 h, 97%; n) 1. mCPBA, $CHCl_3$, 61 °C, 20 h, 40%; 2. NBS, acetic acid, H_2SO_4, rt, 17 h, 64%; o) 1. BuLi, THF, -78 °C, 15 min; 2. Bu_3SnCl, THF, -78 °C – rt, 15 min; 3. $Pd(PPh_3)_4$, **26**, toluene/DMF (5:1), 75 °C, 3 d, 56% over 3 steps; p) 1. TBAF, THF, AcOH, 0 °C – rt, 90 min, 67%; 2. Diglycolic anhydride, Et_3N, THF, 60 °C, 30 min, 85%.

The synthesis of most relevant isostere **2** was more demanding because the trifluoromethyl acceptors affected reactivities strongly, thus many of above procedures did not work. The trifluoromethyl group could ultimately be installed with Weinreb amide **18**, which afforded the mostly inactivated, fully hydrated form of diketone **19**. Diketone **19** could be alternatively synthesized by a Ruppert-Prakash reaction with dialdehyde **9** followed by a Dess-Martin oxidation. The less hydrated mixture with diketone **19** obtained under these aprotic conditions cyclized with thiols **11** and **20** (readily prepared from chloride **21**)[12] into a statistical mixture of products including the desired **22**. This less elegant strategy to install the cyano group already in the condensation step was unavoidable because of failures to introduce cyano or aldehyde groups into electron-poor bistrifluoromethyl DTTs. Treatment of the reaction mixture including **22** with base lead to the hydrolysis of both ester and nitrile into carboxylic acid and amide (and not further), respectively, without preference for one or another even when milder conditions with one equivalent of base were employed. Decarboxylation of the resulting acid **23** followed by regeneration the cyano group by refluxing in $POCl_3$ gave DTT **24**. Oxidation of the sulfur bridge with mCPBA and subsequent bromination with NBS afforded DTT acceptor **25**, ready for Stille coupling with the previously reported DTT donor **26**. Deprotection of the resulting hydrophobic flipper **2'** was unproblematic, but Williamson ether synthesis failed in the presence

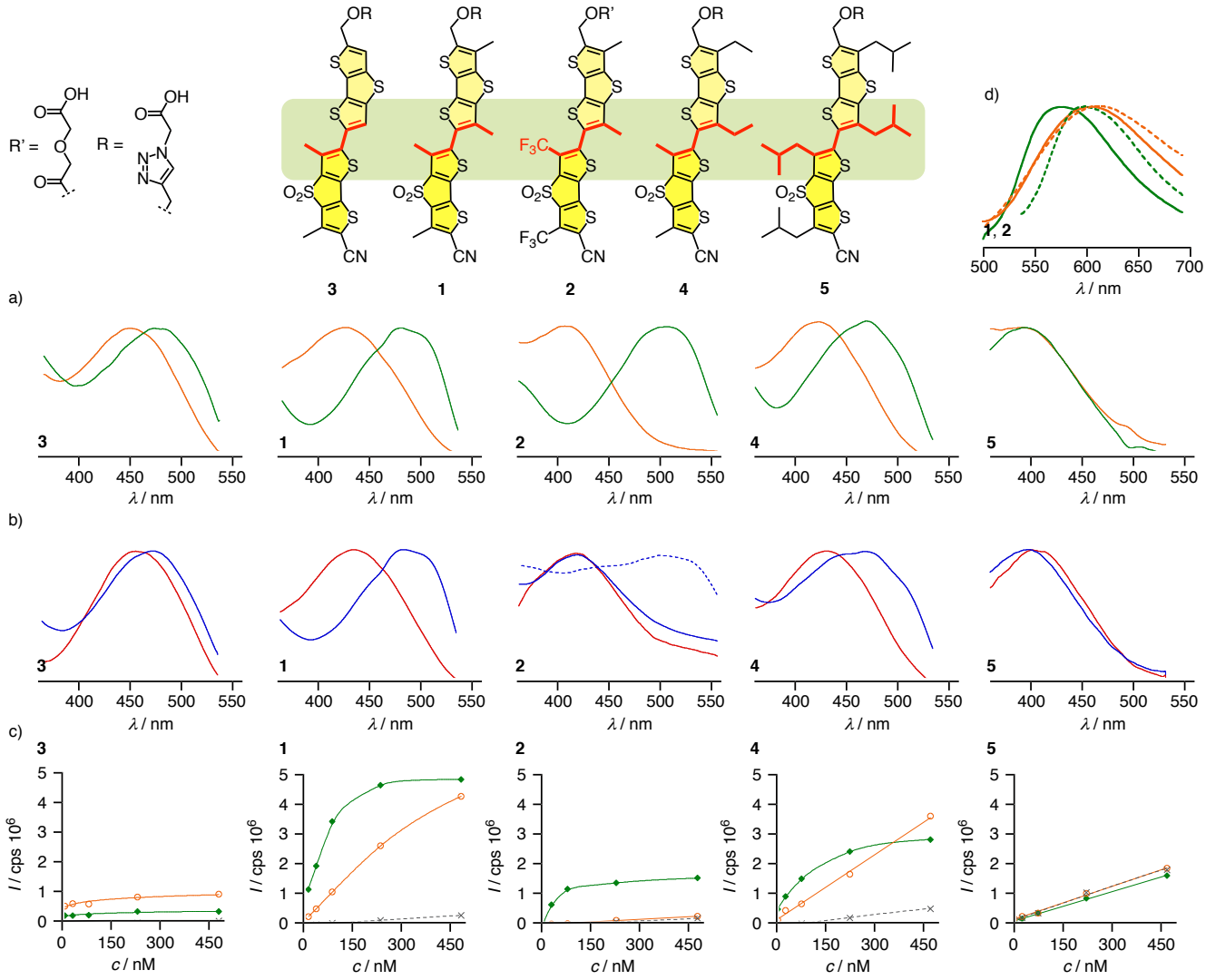

Figure 2. Normalized excitation spectra of **3**, **1**, **2**, **4** and **5** (left to right, λ_{em} in Table S1, 1 μM for **2** in DOPC (due to weak fluorescence), 100 nM for the others) in a) L_d (orange, DOPC LUVs, 75 μM lipid) and L_o membranes (green, SM/CL 7:3) and in b) L_d (red, DPPC, 55 ºC) and S_o membranes (blue, DPPC, 25 ºC, dashed: added at 55 ºC and then cooled to 25 ºC), with c) fluorescence emission intensity as a function of probe concentration in L_d (orange, ○), L_o LUVs (green, ◆) and buffer (grey, X). d) Emission spectra of **1** (solid) and **2** (dashed, λ_{ex} in Table S1, 1 μM for **2** in DOPC, 100 nM for the others) in L_d (orange, DOPC) and L_o LUVs (green, SM/CL

7:3). DOPC: dioleoyl-*sn*-glycero-3-phosphocholine; DPPC: dipalmitoyl-*sn*-glycero-3-phosphocholine; SM: egg sphingomyelin; CL: cholesterol; LUVs: large unilamellar vesicles.

Table 1. Flipper characteristics

cpd[a]	λ_{Lo00} ($\lambda_{\underline{Lo}}$) / nm[b]	τ_{Lo} / ns[c]	$\lambda_{\underline{Ld}}$ / nm[d]	τ_{Ld} / ns[e]	$\Delta\lambda_{Lo00\text{-}\underline{Ld}}$ ($\Delta\lambda_{\underline{Lo}\text{-}\underline{Ld}}$) / nm[f]	I_{Lo}/I_{Ld}[g]	τ_{Lo}/τ_{Ld}[h]	Φ_{Lo} / %[i]	Φ_{Lb} / %[j]	E_{rot} / kJ/mol[k]	$\lambda_{\underline{Lb}}$ / nm[l]	μ_L / D[m]
1	514 (489)	5.54	430	2.92	+84 (+59)	3.1	1.9	49	16	17.4	415	13.8
2[n]	533 (509)	4.36	413	0.79	+120 (+96)	12.7	5.5	44	3.5	20.4	420	18.4
3	478 (479)		454		+24 (+25)	0.5		21	41	5.0	450	
4	518 (470)		425		+93 (+45)	2.1		35	16	16.9	411	
5	404 (403)		403		+1 (0)	1.0		7	6.8	22.8	401	

[a] Compounds, see Figure 2. [b] $\lambda_{Lo}00$, maximum of the 0-0 transition band ($\lambda_{\underline{Lo}}$, average maximum in excitation spectra assigned as center of the band at $I/I_0 = 0.95$) in L_o membranes (SM/CL 7:3 LUVs). [c] τ_{Lo}, average fluorescence lifetime in L_o membranes (SM/CL 7:3 GUVs). [d] $\lambda_{\underline{Ld}}$, average maximum in excitation spectra in L_d membranes (DOPC LUVs). [e] τ_{Lo}, average fluorescence lifetime in L_d membranes (DOPC GUVs). [f] $\Delta\lambda_{Lo}00_{\text{-}\underline{Ld}}$, maximal ($\Delta\lambda_{\underline{Lo}\text{-}\underline{Ld}}$, average) red shift of the excitation maximum from L_d to L_o membranes. [g] Ratio of fluorescence intensity in L_o/L_d LUVs, compared at identical probe concentrations (100 nM, Figure 2c). [h] Ratio of fluorescence lifetime in L_o/L_d GUVs. [i] Estimated maximal fluorescence quantum yield in L_o approximated from Φ_{Lb} x I_{Lo}/I_{Ld}. [j] Fluorescence quantum yield in dioxane as "bulk liquid" (L_b), determined against Nile Red as a standard. [k] Computed rotational energy comparing planarized flippers against the twisted minima. [l] Absorption maximum in 1,4-dioxane (L_b membranes). [m] Transition dipole moment from Lippert-Mataga-Scholte analysis. [n] The different headgroup R' in **2** (Figure 2) has been shown to red shift $\lambda_{\underline{Ld}}$ of **1** by +2 nm and $\Delta\lambda_{\underline{So}\text{-}\underline{Ld}}$ by +5 nm.[15b]

of the trifluoromethyl groups. An alternative headgroup was therefore introduced by a simple acylation with diglycolic anhydride, affording the target amphiphile **2** in good yield (Figure 2). This anionic headgroup has been used previously for the original version of flipper **1**.[13] It is compatible with model studies in LUVs and GUVs but not with cellular imaging, presumably because of decomposition via initial cleavage of the thenyl ester.[4]

Fluorescence in Lipid Bilayer Membranes

The standard assay to assess responsiveness to membrane tension is the comparison of fluorescent properties in liquid-disordered (L_d) and liquid-ordered (L_o) or solid-ordered (S_o) lipid bilayer membranes.[4,8] For the established Flipper-TR® **1**, the lowest energy transition in the excitation spectrum in L_d LUVs did not show any clear vibrational finestructure (Figure 2a, Table 1). The average maximum $\lambda_{\underline{Ld}}$ = 430 nm was defined as the center of the band at 95% intensity. In L_o LUVs, the excitation band increased in intensity (I_{Lo}/I_{Ld} = 3.1 for 100 nM **1**, Figure 2c), red shifted the average maximum to $\lambda_{\underline{Lo}}$ = 489 nm, and showed the emergence of vibrational finestructure (Figure 2a, Table 1). Spectral deconvolution afforded a maximum of $\lambda_{Lo}00$ = 514 nm for the formal 0-0 transition (Figure S4, Tables 1, S4). Deconvolution further revealed the 0-1 maximum at $\lambda_{Lo}01$ = 484 nm and a band at $\lambda_{Lo}E$ = 469 nm which might correspond to a small subpopulation of the probe not well aligned with the lipid tails (Table S4). Thus, the change of the excitation band of original flipper **1** upon transition from L_d to L_o membranes can be characterized by a maximal red shift of $\Delta\lambda_{Lo}00_{-\underline{Ld}}$ = +84 nm, an average red shift $\Delta\lambda_{\underline{Lo}-\underline{Ld}}$ = +59 nm (Table 1), and the 0-1 band red shift $\Delta\lambda_{Lo}01_{-\underline{Ld}}$ = +54 nm.

Compared to original **1**, flipper **3** misses one methyl group next to the twistable bond. As a result, the red shift from L_d to L_o membranes dropped to $\Delta\lambda_{\underline{Lo}\text{-}\underline{Ld}}$ = +25 nm (Figure 2a), in part also because the vibrational finestructure of the L_o band became less resolvable. Additional contributions to this loss in mechanosensitivity originated from a red-shifted $\lambda_{\underline{Ld}}$ = 454 nm, suggesting that reduced repulsion around the twist allowed for partial planarization already in less ordered membranes. Moving from L_d to S_o DPPC membranes, shifts in excitation of flipper **3** further decreased ($\Delta\lambda_{\underline{So}\text{-}\underline{Ld}}$ = +12 nm, Figure 2b), and the fluorescence intensity decreased rather than increased with membrane order (I_{Lo}/I_{Ld} = 0.5, Table 1, Figure 2c). These decreasing shifts together with less resolved finestructures, decreasing, very weak fluorescence intensities (Figure 2c) and poor solubility (*vide infra*) provided consistent support that partitioning of the less twisted flipper **3** into all membranes is poor compared to the more twisted original flipper **1**.

While flipper **3** misses one carbon in the twist region compared to flipper **1**, flipper **4** has one more. The resulting red shifts with increasing membrane order, i.e., $\Delta\lambda_{Lo}00_{\text{-}\underline{Ld}}$ = +93 nm (Figure 2a, Table 1) and $\Delta\lambda_{Lo}01_{\text{-}\underline{Ld}}$ = +65 nm (Table S4) for the formal 0-0 and 0-1 transition, respectively, were slightly superior compared to original **1**. This result was consistent with the lightly enhanced push-pull system of **4**. However, the overall mechanoresponse of **4** was inferior to **1** because of the appearance of an intense blue-shifted band at $\lambda_{Lo}E$ = 452 nm in the deconvoluted spectra that presumably belongs to an important subpopulation of mispositioned **4**. As a consequence, the average $\Delta\lambda_{\underline{Lo}\text{-}\underline{Ld}}$ = +45 nm of **4** that was inferior of $\Delta\lambda_{\underline{Lo}\text{-}\underline{Ld}}$ = +59 nm of **1** (Figure 2a, Table 1). Smaller shifts in S_o DPPC membranes (Figure 2b) and an inversion of I_{Lo}/I_{Ld} values with increasing probe concentration (Figure 2c) further supported that the extra carbon in flipper **4** disturbs partitioning and packing into lipid bilayers. Further crowding around the twist in "leucine" flipper **5** resulted in a total loss of function, as reported previously.[10] Superimposable

dose response curves as well as almost identical excitation and emission spectra in absence or presence of vesicles (Figure S1 and S3) confirmed hindered partitioning as origin of this inactivation (Figure 2c).

An isosteric trifluoromethyl replacement[14] was realized in flipper **2**. The results were unprecedented red shifts of $\lambda_{Lo}00_{\underline{Ld}}$ = +120 nm from L_d to L_o membranes, with λ_{Lo} maxima shifting clearly beyond 500 nm (see below for more detailed discussion) and I_{Lo}/I_{Ld} rising beyond 10 (Figure 2a, c, Table 1). Previous headgroup comparisons in **1** indicate that the different headgroup in **2** will contribute to this record red shift, but these headgroup contributions are minor (**1**: +2 nm for $\lambda_{\underline{Ld}}$, +5 nm for $\Delta\lambda_{\underline{So}\text{-}\underline{Ld}}$).[15b] In S_o DPPC membranes, record red shifts as in L_o SM/CL membranes could be observed only weakly as broadened maxima upon probe addition to L_d DPPC membranes at 55 ºC and cooling down into S_o DPPC membranes (Figure 2b, dashed blue). Direct addition of CF_3 flippers **2** to S_o DPPC membranes at 25 ºC gave blue-shifted spectra, suggesting failure to partition into preformed S_o membranes (Figure 2b, solid blue). Generally reluctant partitioning of CF_3 flipper **2** was confirmed by the compared to CH_3 isostere **1** longer time needed to partition fully into the otherwise unproblematic L_o membranes (Figures 2c, S2).

The record red shift of $\Delta\lambda_{Lo}00_{\underline{Ld}}$ = +120 nm of CF_3 flippers **2** in excitation (Figure 2a) did not coincide with a similar red shift in emission (Figure 2d). As with previous flipper probes, this poor mechanosensitivity confirmed that emission occurs from an always planar excited state[15] and that their mode of action, i.e., planarization in the ground state, differs fundamentally from other established fluorescent membrane probes that operate off-equilibrium in the excited state, including molecular rotors and solvatochromic dyes.[5] Very minor blue shifts of emission with membrane ordering noted for most flippers (Figure S3) could originate from solvatochromism

upon membrane dehydration.[5] This poor solvatochromism of planarized push-pull flippers in membranes could suggest that they are well shielded from water diffusing into disordered membranes, thus supporting their alignment along lipid tails without disturbing their order significantly.[16]

Flipper **2** was compatible with FLIM of GUVs (Figure 3). From L_d to L_o GUVs, FLIM lifetimes increased from τ_{Ld} = 0.79 ns to τ_{Lo} = 4.36 ns (Table 1). The τ_{Lo}/τ_{Ld} = 5.5 increase in lifetime with CF_3 flipper **2** exceeded the τ_{Lo}/τ_{Ld} = 1.9 with the CH_3 original **1**[4,6] significantly (Table 1). This increased mechanosensitivity with regard to FLIM lifetimes corresponded well with the I_{Lo}/I_{Ld} = 12.7 of CF_3 isostere **2** exceeding the I_{Lo}/I_{Ld} = 3.1 of CH_3 isostere **1** clearly, and, of course, the record red shift of $\Delta\lambda_{Lo}00_{\underline{Ld}}$ = +120 nm upon planarization of CF_3 isostere **2**.

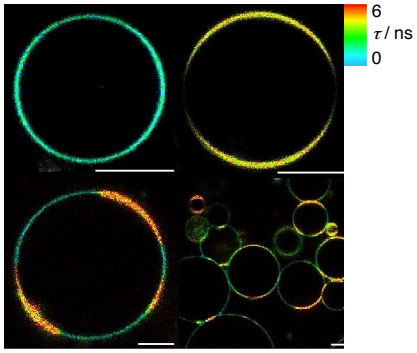

Figure 3. FLIM images of **2** in (top) DOPC (left) and SM/CL (7:3) (right) GUVs, 1 μM, and in (bottom) phase-separated DOPC/SM/CL/**2** (58:25:17:1), scale bar: 10 μm.

Characteristics in Solution and *in Silico*

Flippers **1**–**5** were further characterized in solution or "bulk liquid (L_b) membranes." Whereas the bulkiest flipper **5** provided the most blue-shifted absorption, the absorption maximum of flipper **3** was $\Delta\lambda_{Lb}$ = 30–50 nm red shifted compared to the rest (Figure 4a, Table 1). This red shift supported that the removal of one methyl in the twist region allows for partial flipper planarization already in solution. Despite the different degrees of twist in the ground state, the almost identical emission spectra found for these probes additionally supported that emission occurs from a planar state.[15]

Due to the amphiphilic nature of the flippers, their solvatochromic behavior was evaluated with their hydrophobic precursors **1'** and **2'**. Like for all other flippers, the absorption maxima of CF_3 flipper **2'** was nearly solvent independent (Figure 4b, solid). This negligible solvatochromism in the absorption spectra was consistent with the decoupling of the push-pull system by twisting and was further supported by visualization of the HOMO and LUMO orbitals of twisted and planarized probes with DFT calculations (see below, Figure 5). The emission maxima of CF_3 flipper **2'** showed very important positive solvatochromism. This maximal solvatochromism in emission in solution (Figure 4b, dashed) was in clear contrast to the minimal solvatochromism in membranes (Figure 2d), thus supporting that the latter originates from "waterproof" alignment along lipid tails.

Lippert-Mataga analysis of the solvatochromism in solution gave, including the Scholte correction,[17] a transition dipole moment μ_L = 18.4 D for isostere **2'** that exceeded the μ_L = 13.8 D of original **1'** clearly (Figures S9, S10). An operational push-pull system was supported by the electronic structure computed for the HOMO with electron density on the donating flipper (Figure 5a, b, left) and the LUMO with charge density transferred intramolecularly to the accepting flipper (Figure 5a, b, right).

The increased push-pull dipole of excited-state planarized flipper **2'** compared to **1'** was consistent with the substitution of weak methyl donors (Hammett σ_p^+ = –0.31. σ_p = –0.17) by strong trifluoromethyl acceptors (σ_p^+ = +0.61, σ_p = +0.54; cyano: $\sigma_p^+ = \sigma_p$ = +0.66).[18] These strong trifluoromethyl acceptors were well reflected in the energy of the first LUMO of the cyano intermediate **25** (Scheme 1). It was found, according to differential pulse voltammetry (DPV), at E_{LUMO} –3.84 eV against E_{LUMO} –5.10 eV for the Fc^+/Fc couple (Figure S11). This value is far below dialkyl monocyano DTTO2s (E_{LUMO} –3.30 eV), and also below dicyano DTTO2s (E_{LUMO} –3.70 eV).[19]

Fluorination of the original flipper **1** increased the computed rotational barrier around the twistable bond between the two flippers from E_{rot} = +17.4 to E_{rot} = +20.4 kJ mol^{-1} (M06-2X/6-311G(d,p), gas phase; Figure 4d). This increase was consistent with repulsion between the methyl fluorines on the accepting flipper and the electron-rich sulfur on the donating flipper in **2** (Figure 4e). S-F repulsion rather than attraction in CF_3 flipper **2** implied that in CH_3 isostere **1**, the corresponding S-H contact could also be attractive rather than repulsive because the σ holes[19,20] on electron-rich sulfur on the donating flipper are too shallow to repel the hydrogens strongly (Figure 4e). The small difference in rotational energy between the two isosteres further supported that repulsion between the deep σ holes on electron-poor sulfur on the accepting flipper and the methyl hydrogens on the donating flipper mostly account for the deplanarization of both mechanophores.

This increased twisting in CF_3 isostere **2** compared to the CH_3 original **1** could conceivably contribute to the blue-shifted excitation maximum at $\lambda_{\underline{Ld}}$ = 413 nm compared to $\lambda_{\underline{Ld}}$ = 430 nm in L_d membrane (Figure 2a). Upon planarization in L_o membranes, this blue shift with CF_3 flipper **2** compared to CH_3 flipper **1** inverted into a red shift for the CF_3 isostere **2**, that is $\lambda_{Lo}00$ = 533

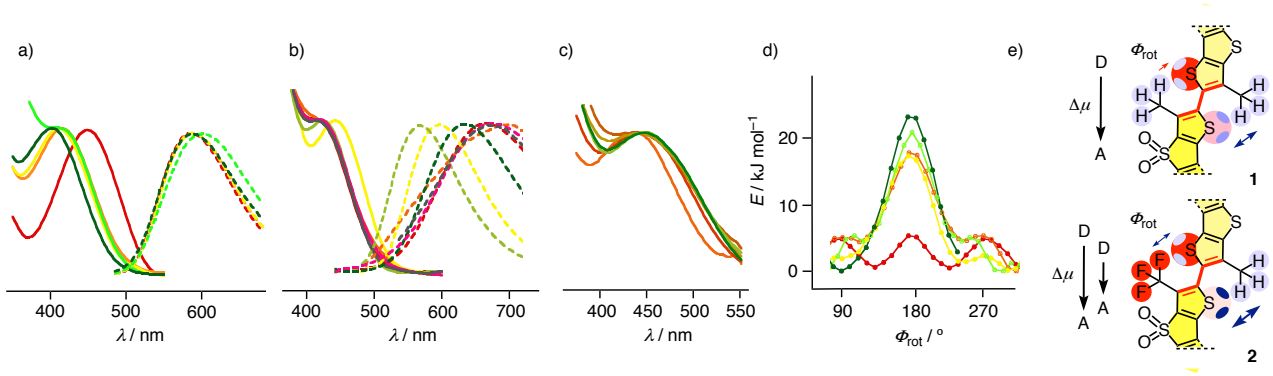

Figure 4. a) Normalized absorption (left) and emission (right) spectra of **1** (orange), **2** (light green), **3** (red), **4** (yellow) and **5** (dark green) in dioxane. b) Normalized absorption (solid) and emission (dashed) spectra of **2'** (Scheme 1) in pentane (light green), toluene (yellow), Et_2O (dark green), EtOAc (red), THF (magenta), dimethoxyethane (grey), DMSO (orange). c) Normalized excitation spectra of **2** in ethyleneglycol in the presence of 0% (orange, 20.8 cP), 20% (red), 30% (brown) 40% (khaki), 60% (light green), 80% glycerol (dark green, 620.7 cP). d) Computed energies as a function of twist angle between the two aromatic planes for the corresponding methyl-esters **1''**–**5''** of probes **1** (orange), **2** (light green), **3** (red), **4** (yellow) and **5** (dark green). e) Nature of the twists in **1** and **2**, see text.

nm ($\lambda_{Lo}01$ = 498 nm, $\lambda_{\underline{Lo}}$ = 509 nm), compared to $\lambda_{Lo}00$ = 514 nm ($\lambda_{Lo}01$ = 484 nm, $\lambda_{\underline{Lo}}$ = 489 nm) for the CH_3 original **1**. This inversion testified for the emergence of the enhanced push-pull system in CF_3 flipper **2**, as indicated by the increased solvatochromism of the emission maximum. The two effects then added up to the record red shift of $\Delta\lambda_{Lo}00_{\underline{Ld}}$ = +120 nm ($\Delta\lambda_{\underline{Lo}-\underline{Ld}}$ = +96 nm), that is record mechanosensitivity, for CF_3 flipper **2** moving from L_o to L_d membranes. In clear contrast, increasing viscosity in solution[5] caused only marginal shifts of the excitation maximum of CF_3 flipper **2'** (Figure 4c). This control supported that the red-shifted

excitation of flipper probes in membranes of increasing order originates from mechanical planarization in equilibrium in the ground state, and not from off-equilibrium kinetics.[15,21] Contrary to original flipper **1**, fluorescence intensities of CF_3 isostere **2** increased with increasing viscosity (Figures S5, S6). Consistent with previous observations with leucine flipper **5**,[10] this opposing behavior could indicate that with more twisted ground state and higher rotational barrier (Figure 4d, e), the FC excited state of **2** could increasingly relax toward the fully twisted, non-emissive TICT-like excited state of "molecular rotors"[5] rather than toward the fully planarized, highly emissive ICT-like excited state of planarized push-pull probes[15] (FC: Franck Condon; TICT, twisted intramolecular charge transfer; ICT, intramolecular charge transfer).

The fluorescence quantum yield of CF_3 flipper **2** in dioxane, measured against Nile Red (70%) as a standard, was with Φ_{Lb} = 3.5% indeed very weak (Table 1, Figure S7). Quantum yields in solution generally decreased with increasing rotational barrier, from the decrowded H flipper **3** with Φ_{Lb} = 41% against E_{rot} = 5.0 kJ/mol to the overcrowded "leucine" flipper **5** with Φ_{Lb} = 6.8% against E_{rot} = 22.8 kJ/mol (Figure S8). This trend was consistent with the existence of competing twisted (dark) and planar (bright) excited states that was deduced above from the opposing dependence **1** and **2** on viscosity (Figure S6). The strong increase of fluorescence intensity I_{Lo}/I_{Ld} = 12.7 and lifetime τ_{Lo}/τ_{Ld} = 5.5 suggested that the formal quantum yield of planarized CF_3 flipper **2** in L_o membranes should be much higher, up to Φ_{Lo} = 44% (Table 1) if the same absorption coefficients for both planar and twisted form of the probe are considered. This was in the range of Φ_{Lo} = 49% approximated for CH_3 original **1**, which shows much less pronounced I_{Lo}/I_{Ld} = 3.1 and τ_{Lo}/τ_{Ld} = 1.9 (Table 1). Higher mechanosensitivity of **2** compared to **1** also with regard to fluorescence intensity and lifetime was again consistent with the existence of competing twisted (dark)[10] and planar (bright)[15] excited states. Namely, increasing planarization in the ground state will result in increasingly planar FC excited states and thus

decreasing losses from relaxation into fully twisted, non-emissive TICT-like excited states of **2**. This record mechanosensitivity with regard not only to red-shifted excitation but also to fluorescence intensity and lifetime, suggested that CF_3 flipper **2** could, in principle, outperform CH_3 original **1** as fluorescent membrane tension probe[6,8] in living cells.

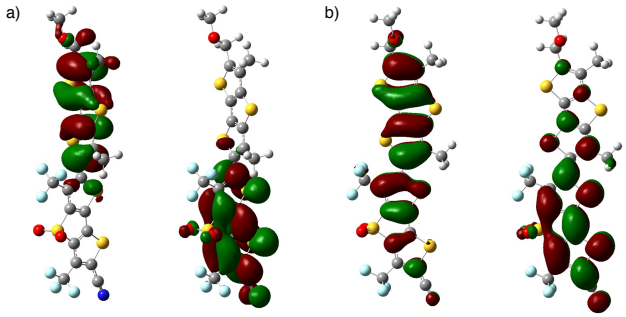

Figure 5. HOMO (left) and LUMO (right) orbitals obtained from DFT (M06-2X/6-311G(d,p), gas phase) calculations for a corresponding methyl-ether **2''** (Figure S12) of probe **2**, S-C-C-S dihedral angle a) 90° (twisted), b) 180° (planarized).

Conclusions

The lessons learned from comprehensive twist engineering of flipper probes are that a) every atom matters, b) red shifts up to +120 nm are accessible, and c) fluorescence quantum yields can be generally rationalized as a result of kinetic competition between bright, fully planarized ICT and dark, fully twisted TICT excited states. Removal of one carbon in the twist region of dithienothiophenes push-pull dimers yields bright probes that planarize already in the absence of forces. Addition of one carbon in the twist region already hinders non-interfering alignment along lipid tails in lipid membranes, a mismatch that rapidly escalates with increasing bulk in the twist region. Substitution of one methyl by an isosteric trifluoromethyl in the twist region produces record red shifts well over +100 nm of the excitation maxima with increasing

membrane order. This maximized mechanosensitivity is shown to originate from a combination of increased deplanarization in the absence and increased polarization in the presence of spacial confinement. Consistent with competing planar (bright) and twisted (dark) excited states, this red-shifted excitation upon planarization in the ground state coincides with record increases in fluorescence intensity and lifetime.

However, increased push-pull power in planar conformation comes inevitably with increased fragility in twisted conformation. Although all spectroscopic data suggest that the new flipper **2** should outperform original **1** as fluorescent membrane tension probe in living cells, FLIM with **2** in cells is inconceivable for this reason. This "flipper dilemma," i.e., strong donors and acceptors needed for red shifts in planar conformation but incompatible with the twisted resting state, calls for donors and acceptors that turn on only upon planarization.[15,22] Ongoing, promising progress in this direction will be published in due course.[22]

Experimental Section

Experimental details can be found in the Supporting Information.

Acknowledgements

We thank Mariano Macchione for contributions to synthesis, Aurélien Roux and Adai Colom for assistance, the NMR, the MS and the bioimaging platforms for services, and the University of Geneva, the Swiss National Centre of Competence in Research (NCCR) Chemical Biology, the NCCR Molecular Systems Engineering and the Swiss NSF for financial support.

Keywords: fluorescent probes • membrane tension • mechanochemistry • force imaging • chalcogen bonds • torsion angle

[1] a) M. Krieg, G. Fläschner, D. Alsteens, B. M. Gaub, W. H. Roos, G. J. L. Wuite, H. E. Gaub, C. Gerber, Y. F. Dufrêne, D. J. Müller, *Nat. Rev. Phys.* **2019**, *1*, 41–57; b) B. Pontes, P. Monzo, N. C. Gauthier, *Semin. Cell Dev. Biol.* **2017**, *71*, 30–41; c) P. Roca-Cusachs, V. Conte, X. Trepat, *Nat. Cell Biol.* **2017**, *19*, 742–751.

[2] a) A. Fin, A. Vargas Jentzsch, N. Sakai, S. Matile, *Angew. Chem. Int. Ed.* **2012**, *51*, 12736–12739; b) M. Macchione, M. Tsemperouli, A. Goujon, A. R. Mallia, N. Sakai, K. Sugihara, S. Matile, *Helv. Chim. Acta* **2018**, *101*, e1800014; c) K. Strakova, S. Soleimanpour, M. Diez-Castellnou, N. Sakai, S. Matile, *Helv. Chim. Acta* **2018**, *101*, e1800019.

[3] a) A. P. Gamiz-Hernandez, I. N. Angelova, R. Send, D. Sundholm, V. R. I. Kaila, *Angew. Chem. Int. Ed.* **2015**, *54*, 11564–11566; b) S. Begum, M. Cianci, B. Durbeej, O. Falklöf, A. Hädener, J. R. Helliwell, M. Helliwell, A. C. Regan, C. I. F. Watt, *Phys. Chem. Chem. Phys.* **2015**, *17*, 16723–16732; c) B. Baumeister, S. Matile, *Chem. Eur. J.* **2000**, *6*, 1739–1749.

[4] a) S. Soleimanpour, A. Colom, E. Derivery, M. Gonzalez-Gaitan, A. Roux, N. Sakai, S. Matile, *Chem. Commun.* **2016**, *52*, 14450–14453; b) K. Strakova, L. Assies, A. Goujon, F. Piazzolla, H. V. Humeniuk, S. Matile, *Chem. Rev.*, in press, DOI: 10.1021/acs.chemrev.9b00279.

[5] a) A. S. Klymchenko, *Acc. Chem. Res.* **2017**, *50*, 366–375; b) J. E. Chambers, M. Kubánková, R. G. Huber, I. López-Duarte, E. Avezov, P. J. Bond, S. J. Marciniak, M. K. Kuimova, *ACS Nano* **2018**, *12*, 4398–4407; c) R. U. Kulkarni, M. Vandenberghe, M. Thunemann, F. James, O. A. Andreassen, S. Djurovic, A. Devor, E. W. Miller, *ACS Cent. Sci.* **2018**, *4*, 1371–1378; d) Y. Xiong, A. Vargas Jentzsch, J. W. M. Osterrieth, E. Sezgin, I. V. Sazanovich, K. Reglinski, S. Galiani, A. W. Parker, C. Eggeling, H. L. Anderson, *Chem. Sci.* **2018**, *9*, 3029–3040; e) E. A. Halabi, S. Püntener, P. Rivera-Fuentes, *Helv. Chim. Acta* **2018**, *101*, e1800165; f) E. Sezgin, F. B. Can, F. Schneider, M. P. Clausen, S. Galiani, T.

A. Stanly, D. Waithe, A. Colaco, A. Honigmann, D. Wüstner, F. Platt, C. Eggeling, *J. Lipid Res.* **2016**, *57*, 299–309; g) A. Jiménez-Sánchez, E. K. Lei, S. O. Kelley, *Angew. Chem. Int. Ed.* **2018**, *57*, 8891–8895; h) J. Yin, M. Peng, W. Lin, *Anal. Chem.* **2019**, *91*, 8415−8421; i) C. W. T. Leung, Y. Hong, S. Chen, E. Zhao, J. W. Y. Lam, B. Z. Tang, *J. Am. Chem. Soc.* **2013**, *135*, 62–65; j) Z. Yang, Y. He, J.-H. Lee, N. Park, M. Suh, W.-S. Chae, J. Cao, X. Peng, H. Jung, C. Kang, J. S. Kim, *J. Am. Chem. Soc.* **2013**, *135*, 9181–9185; k) P. Yan, A. Xie, M. Wei, L. M. Loew, *J. Org. Chem.* **2008**, *73*, 6587–6594; l) Y. Niko, P. Didier, Y. Mely, G. Konishi, A. S. Klymchenko, *Sci. Rep.* **2016**, *6*, 1–9; m) T. Baumgart, G. Hunt, E. R. Farkas, W. W. Webb, G. W. Feigenson, *Biochim. Biophys. Acta* **2007**, *1768*, 2182–2194; n) I. A. Karpenko, M. Collot, L. Richert, C. Valencia, P. Villa, Y. Mély, M. Hibert, D. Bonnet, A. S. Klymchenko, *J. Am. Chem. Soc.* **2015**, *137*, 405–412; o) M. Kubánková, I. López-Duarte, D. Kiryushko, M. K. Kuimova, *Soft Matter* **2018**, *14*, 9466–9474; p) M. A. Haidekker, E. A. Theodorakis, *J. Mater. Chem. C* **2016**, *4*, 2707–2718; q) C. Bauer, R. Duwald, G. M. Labrador, S. Pascal, P. Moneva Lorente, J. Bosson, J. Lacour, J.-D. Rochaix, *Org. Biomol. Chem.* **2018**, *16*, 919–923; r) V. Grenier, B. R. Daws, P. Liu, E. W. Miller, *J. Am. Chem. Soc.* **2019**, *141*, 1349–1358; s) H. Dube, M. R. Ams, J. Rebek, *J. Am. Chem. Soc.* **2010**, *132*, 9984–9985; t) M. Collot, T. K. Fam, P. Ashokkumar, O. Faklaris, T. Galli, L. Danglot, A. S. Klymchenko, *J. Am. Chem. Soc.* **2018**, *140*, 5401–5411; u) L. Peterhans, E. Alloa, Y. Sheima, L. Vannay, M. Leclerc, C. Corminboeuf, S. C. Hayes, N. Banerji, *Phys. Chem. Chem. Phys.* **2017**, *19*, 28853—28866.; v) T. Muraoka, K. Umetsu, K. V. Tabata, T. Hamada, H. Noji, T. Yamashita, K. Kinbara, *J. Am. Chem. Soc.* **2017**, *139*, 18016–18023; w) R. D. Ortuso, U. Cataldi, K. Sugihara, *Soft Matter* **2017**, *13*, 1728–1736; x) M. E. Cinar, T. Ozturk, *Chem. Rev.* **2015**, *115*, 3036–3140; y) G. Barbarella, F. Di Maria, *Acc. Chem. Res.* **2015**, *48*, 2230–2241; z) M. Mauro, A. Aliprandi, D. Septiadi, N. S. Kehr, L. De Cola, *Chem. Soc.*

Rev. **2014**, *43*, 4144–4166; aa) Y.-M. Zhang, X.-J. Zhang, X. Xu, X.-N. Fu, H.-B. Hou, Y. Liu, *J. Phys. Chem. B* **2016**, *120*, 3932−3940; bb) X.-M. Chen, Y. Chen, Q. Yu, B.-H. Gu, Y. Liu, *Angew. Chem. Int. Ed.* **2018**, *57*, 12519 –12523.

[6] A. Colom, E. Derivery, S. Soleimanpour, C. Tomba, M. D. Molin, N. Sakai, M. González-Gaitán, S. Matile, A. Roux, *Nat. Chem.* **2018**, *10*, 1118–1125.

[7] a) J. C. S. Ho, P. Rangamani, B. Liedberg, A. N. Parikh, *Langmuir* **2016**, *32*, 2151–2163; b) T. Hamada, Y. Kishimoto, T. Nagasaki, M. Takagi, *Soft Matter* **2011**, *7*, 9061–9068.

[8] A. Goujon, A. Colom, K. Straková, V. Mercier, D. Mahecic, S. Manley, N. Sakai, A. Roux, S. Matile, *J. Am. Chem. Soc.* **2019**, *141*, 3380–3384.

[9] M. Riggi, C. Bourgoint, M. Macchione, S. Matile, R. Loewith, A. Roux, *J. Cell Biol.* **2019**, *218*, 2265–2276.

[10] M. Macchione, N. Chuard, N. Sakai, S. Matile, *ChemPlusChem* **2017**, *82*, 1062–1066.

[11] J. Frey, A. D. Bond, A. B. Holmes, *Chem. Commun.* **2002**, 2424–2425.

[12] S. R. Alexander, A. J. Fairbanks, *Org. Biomol. Chem.* **2016**, *14*, 6679–6682.

[13] M. Dal Molin, Q. Verolet, A. Colom, R. Letrun, E. Derivery, M. Gonzalez-Gaitan, E. Vauthey, A. Roux, N. Sakai, S. Matile, *J. Am. Chem. Soc.* **2015**, *137*, 568–571.

[14] a) G. A. Patani, E. J. LaVoie, *Chem. Rev.* **1996**, *96*, 3147-3176; b) E. N. G. Marsh, *Acc. Chem. Res.* **2014**, *47*, 2878–2886; c) N. A. Meanwell, J. Med. Chem. 2011, 54, 2529−2591; d) S. Purser, P. R. Moore, S. Swallow, V. Gouverneur, *Chem. Soc. Rev.* **2008**, *37*, 320–330; e) C.-J. Chaing, J.-C. Chen, Y.-J. Kuo, H.-Y. Tsao, K.-Y. Wu, C.-L. Wang, *RSC Adv.* **2016**, *6*, 8628–8638; f) Y Zhou, J. Wang, Z. Gu, S. Wang, W. Zhu, J. L. Aceña, V. A. Soloshonok, K. Izawa, H. Liu, *Chem. Rev.* **2016**, *116*, 422−518.

[15] a) Q. Verolet, A. Rosspeintner, S. Soleimanpour, N. Sakai, E. Vauthey, S. Matile, *J. Am. Chem. Soc.* **2015**, *137*, 15644–15647; b) Q. Verolet, M. Dal Molin, A. Colom, A. Roux, L. Guénée, N. Sakai, S. Matile, *Helv. Chim. Acta* **2017**, *100*, e1600328.

[16] F. Neuhaus, F. Zobi, G. Brezesinski, M. Dal Molin, S. Matile, A. Zumbuehl, *Beilstein J. Org. Chem.* **2017**, *13*, 1099–1105.

[17] C. C. Vequi-Suplicy, K. Coutinho, M. T. Lamy, *Biophys. Rev.* **2014**, *6*, 63–74.

[18] C. Hansch, A. Leo, R. W. Taft, *Chem. Rev.* **1991**, *91*, 165–195.

[19] S. Benz, J. López-Andarias, J. Mareda, N. Sakai, S. Matile, *Angew. Chem. Int. Ed.* **2017**, *56*, 812–815.

[20] a) A. Bauzá, T. J. Mooibroek, A. Frontera, *ChemPhysChem* **2015**, *16*, 2496–2517; b) B. R. Beno, K.-S. Yeung, M. D. Bartberger, L. D. Pennington, N. A. Meanwell, *J. Med. Chem.* **2015**, *58*, 4383–4438; c) L. Vogel, P. Wonner, S. M. Huber, *Angew. Chem. Int. Ed.* **2019**, *58*, 1880–1891; d) G. E. Garrett, G. L. Gibson, R. N. Straus, D. S. Seferos, M. S. Taylor, *J. Am. Chem. Soc.* **2015**, *137*, 4126–4133; e) K. T. Mahmudov, M. N. Kopylovich, M. F. C. Guedes da Silva, A. J. L. Pombeiro, *Dalton Trans.* **2017**, *46*, 10121–10138; f) Y. Zhao, Y. Cotelle, N. Sakai, S. Matile, *J. Am. Chem. Soc.* **2016**, *138*, 4270–4277; g) S. Benz, C. Besnard, S. Matile, *Helv. Chim. Acta* **2018**, *101*, e1800075; h) J. Y. C. Lim, P. D. Beer, *Chem* **2018**, *4*, 731–783; i) P. Scilabra, G. Terraneo, G. Resnati**,** *Acc. Chem. Res.* **2019**, *52*, 1313–1324; j) H. Huang, L. Yang, A. Facchetti, T. J. Marks, *Chem. Rev.* **2017**, *117*, 10291–10318; k) D. J. Pascoe, K. B. Ling, S. L. Cockroft, *J. Am. Chem. Soc.* **2017**, *139*, 15160–15167; l) S. Scheiner, *Chem. – Eur. J.* **2016**, *22*, 18850–18858; m) M. R. Ams, N. Trapp, A. Schwab, J. V. Milić, F. Diederich, *Chem. Eur. J.* **2019**, *25*, 323–333; n) N. Biot, D. Bonifazi, *Chem. Eur. J.* **2018**, *24*, 5439–5443; o) L. Chen, J. Xiang, Y. Zhao, Q. Yan, *J. Am. Chem. Soc.* **2018**, *140*, 7079–7082; p) H. Zhao, F. P. Gabbaï, *Nat. Chem.* **2010**, *2*, 984–990.

[21] H. V. Humeniuk, A. Rosspeintner, G. Licari, V. Kilin, L. Bonacina, E. Vauthey, N. Sakai, S. Matile, *Angew. Chem. Int. Ed.* **2018**, *57*, 10559–10563.

[22] M. Macchione, A. Goujon, K. Strakova, H. V. Humeniuk, G. Licari, E. Tajkhorshid, N. Sakai, S. Matile, *Angew. Chem. Int. Ed.*, in press.